THE JOURNAL OF PHYSICAL CHEMISTRY C

ARTICLE

pubs.acs.org/JPCC

Pressure-Induced Structural Transformations of ZnO Nanowires Probed by X-ray Diffraction

Zhaohui Dong,[†] Kirill K. Zhuravlev,[†] Stephen A. Morin,[‡] Linsen Li,[‡] Song Jin,[‡] and Yang Song*[,†]

[†]Department of Chemistry, The University of Western Ontario, London, Ontario N6A 5B7, Canada

[‡]Department of Chemistry, University of Wisconsin-Madison, 1101 University Avenue, Madison, Wisconsin 53706, United States

ABSTRACT: ZnO nanowires were investigated at high pressures of up to 27 GPa in situ in a diamond anvil cell using synchrotron X-ray diffraction. Upon compression, a wurtzite-to-rocksalt phase transformation was observed, but both the onset and the completion pressures of this transformation were enhanced compared with all previously studied morphologies of ZnO, including nanocrystals and their bulk counterparts. Upon decompression, the rocksalt phase was found to sustain at near ambient pressure and could be recovered in a significant amount. Moreover, the pressure−volume equations of state for both the wurtzite and the rocksalt phases indicate that their bulk moduli are significantly higher than those of bulk ZnO and nanocrystals. The SEM images of the ZnO nanowires both before and after the compression suggest the pressure-induced morphology modifications, corroborating the understanding of other structure and property evolutions with pressure. Finally, possible pressure-induced phase transition mechanisms were explored by examining the cell parameters and the internal structural parameter with pressures.

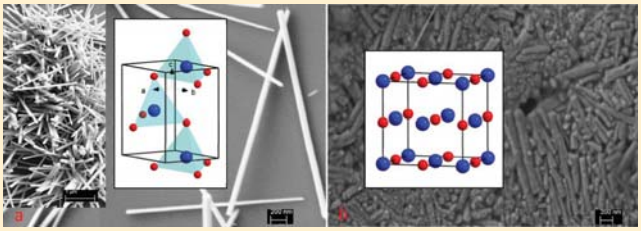

INTRODUCTION

As an important wide band gap semiconductor (E_g = 3.37 eV), ZnO has a wide range of applications, such as in piezoelectric transducers, chemical sensors, optical coatings, photovoltaics, and ceramics.[1−3] In contrast to the corresponding bulk counterparts, nanostructured ZnO has enhanced electronic, and photoconducting properties.[4,5] Because of the unique crystal quality and photonic properties, in particular, 1D ZnO nanomaterials have been used as functional units in the fabrication of electronic, piezoelectronic, electrochemical, and highly sensitive gas sensors with nanoscale dimensions.[6−8] Therefore, an increasing research effort has been focused on nanostructured ZnO, especially in exploring new structures, properties, as well as synthetic methods. In addition to the traditional synthetic and fabrication routes, external pressure can provide an alternative effective driving force to tune the structures and thus the properties of the nanostructured materials.[9] Therefore, investigations of the structural and phase transformations of nanomaterials under high pressure represent a prevailing materials research frontier.[10−13] One of the most interesting observations in those studies is that the compressed nanomaterials behave significantly differently than their corresponding bulk counterparts under pressure. For example, our previous studies on 1D nanomaterials (e.g., SnO_2 nanowires and nanobelts,[11] GaN nanowires,[10] and BN nanotubes[12]) have demonstrated profound implications for producing controlled structures by combined pressure−morphology tuning.

Under ambient conditions, ZnO has a wurtzite-type (B4) structure (space group $P6_3mc$) regardless of the morphologies.[14−17] The wurtzite phase transforms to a rocksalt-type (B1) phase (space group $Fm\bar{3}m$) upon compression to some certain threshold pressure (e.g., >8.8 GPa).[18] This B4-to-B1 phase transition in ZnO has been extensively investigated using different experimental and theoretical approaches,[13,14,17,19−25] but the transition pressure varies in a broad range depending on the morphology of ZnO as well as other experimental conditions. For instance, it was well-established that the B4-to-B1 phase transition for bulk ZnO takes place at ∼9 ± 0.2 GPa.[19,23−25] However, the transition pressure for ZnO nanocrystals falls in the broad range from 10.5 to 15.1 GPa as the grain size of the nanocrystals varies from 50 to 12 nm.[13,14,17,20−22]

In contrast to bulk ZnO and nanocrystals, which have been extensively studied, only a few high-pressure studies have been carried out on 1D ZnO so far. Hou et al. reported a high-pressure study on ZnO nanotubes showing that the B4-to-B1 phase transition took place at 10.5 GPa, the same as ZnO nanocrystals with a grain size of 50 nm. However, the pressure at which the transformation is completed (i.e., 18.4 GPa) [16] was significantly higher than that for bulk ZnO[18] and ZnO nanocrystals[21] (i.e., 13 and 15 GPa, respectively). In addition, Yan et al.[26] examined the doped ZnO nanowires with Raman spectroscopy under high pressures. A phase transformation was claimed between 10.3 and 12.2 GPa, but no detailed structural information was provided. The results of all of these high-pressure studies on nanostructured

Special Issue: Chemistry and Materials Science at High Pressures Symposium

Received: June 10, 2011
Revised: August 29, 2011
Published: October 10, 2011

dx.doi.org/10.1021/jp205467h | *J. Phys. Chem. C* 2012, 116, 2102–2107

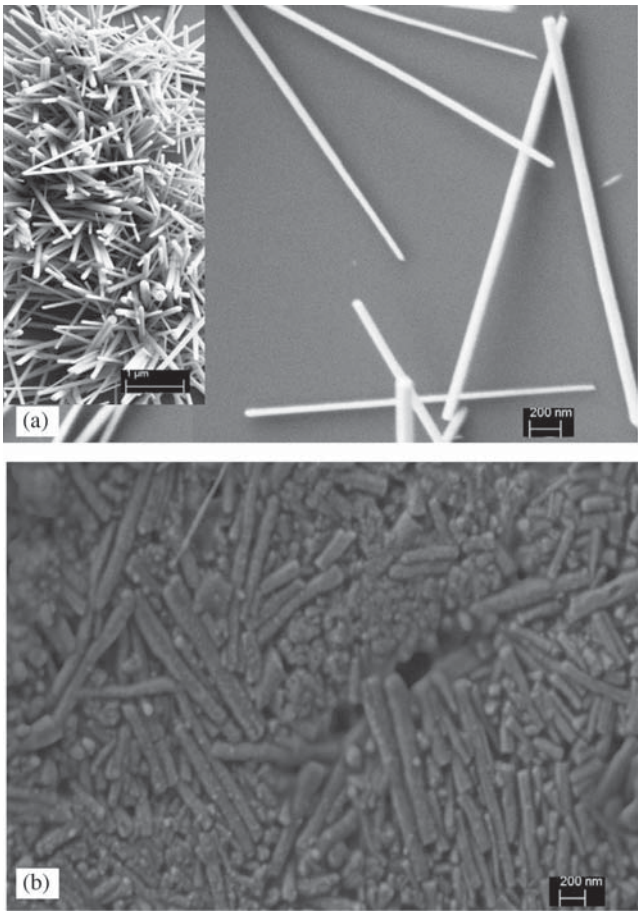

Figure 1. SEM images of ZnO nanowires before (a) and after compression (b). The inset of panel a shows a larger scale image of the nanowires.

ZnO are summarized in Table 1 together with some representative studies on bulk ZnO.

In this Article, we report the first high-pressure study of ZnO nanowires using the synchrotron X-ray diffraction technique. Starting with laboratory synthesized ZnO nanowires, we compressed the nanomaterials to high pressures of up to 26 GPa, followed by decompression. The quantitative analysis of the diffraction patterns revealed new and interesting structural information that allows for the understanding of the high-pressure behavior of ZnO nanowires as well as the associated transition mechanisms.

EXPERIMENTAL SECTION

ZnO nanowires were synthesized in a continuous flow reactor by mixing equimolar precursor solutions of Zn $(NO_3)_3 \cdot (H_2O)_6$ and hexamethylenetetramine (HMT) both at a concentration of 100 μM and a temperature of 95 °C. This catalyst-free growth of nanowires was driven by screw-dislocations,[27] and the detailed apparatus, synthetic procedures, as well as the experimental parameters that control the morphologies of ZnO nanowires have been reported elsewhere.[28] The scanning electron microscopy (SEM) images (Figure 1 a) revealed that the ZnO had a very good wire morphology and uniformity with an average length of 3 to 4 μm and width of 50−100 nm.

High-pressure experiments were performed using a symmetric diamond anvil cell (DAC) equipped with a pair of type-I diamonds

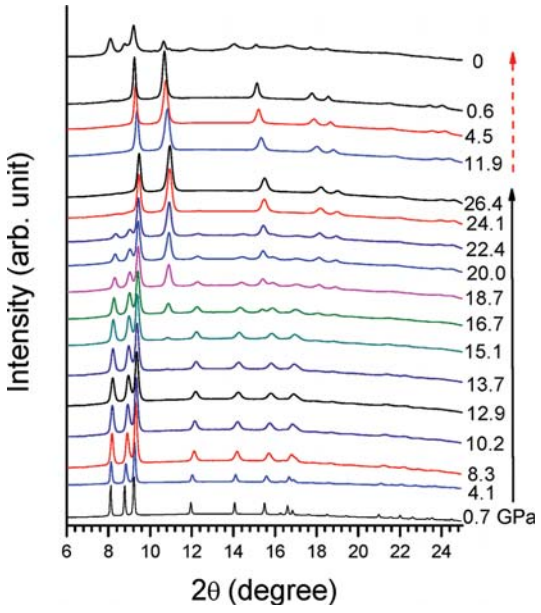

Figure 2. Selected X-ray diffraction patterns of ZnO nanowires upon compression to 26.4 GPa and decompression to ambient pressure. The pressures in gigapascals are labeled. The solid and dashed arrows indicate the compression and decompression sequence, respectively.

with a culet size of 400 μm. A preindented stainless-steel gasket drilled with a 130 μm hole at the center was used as the sample chamber. Neon gas was compressed into the DAC with the sample by a special gas-loading system and was used as the pressure-transmitting medium to maintain the hydrostatic conditions. The pressure was determined by the well-established ruby fluorescence method using an online ruby optical system. A motorized gear box was also employed to regulate the pressure with fine increments.

In situ angle-dispersive X-ray diffraction measurements were carried out at room temperature using the 16ID-B beamline of the HPCAT at the Advanced Photon Source. The incident wavelength of the monochromatic beam was 0.4072 Å with a beam size of to 4 × 5 μm^2 focused at the sample. The diffraction data were recorded on a MAR345 imaging plate with an exposure time of 60 s; then, the 2D Debye−Scherrer diffraction patterns were integrated by using the Fit2D program. A detailed Rietveld analysis was performed using the GSAS package.

RESULTS AND DISCUSSION

X-ray diffraction measurements were performed on ZnO nanowires on compression of up to 26.4 GPa followed by decompression. The selected X-ray patterns are depicted in Figure 2. All diffraction reflections at the near ambient pressure can be indexed to the known B4 structure with lattice constants of $a = b = 3.2517$ Å and $c = 5.2006$ Å, consistent with the previous diffraction measurement of ZnO.[26] Upon compression, the B4 phase was found to persist to 12.9 GPa, as indicated by the consistent indexing of all reflections associated with this phase. At 13.7 GPa, a new reflection appeared at 10.8431° with discernible intensity, which can be indexed as (2 0 0) for the B1 phase, indicating the onset of the wurtzite-to-rocksalt phase transformation. This onset phase transition pressure is significantly higher than that observed in the ZnO nanocrystals, nanotubes, or the

dx.doi.org/10.1021/jp205467h |J. Phys. Chem. C 2012, 116, 2102–2107

Table 1. Summary of High-Pressure Studies of ZnO with Different Morphologies

			B4-to-B1 transition pressure (GPa)				
			compression[a]		decompression	bulk modulus (GPa)	
morphology	dimension	pressure-transmitting medium	P_i	P_c	P	B4 phase	B1 phase
bulk		[b]		8.7	2	183	228
		helium[c]	8.8	12.8	3.2	135	178
		silicon oil[d]	8.9	11.5		154	229
nanocrystal	50 nm[d]	silicon oil	10.5	13		151	221
	12 nm[e]	16:3:1 MeOH-EtOH-H_2O	13.2	17.5	1.7		
nanotube[f]	d: 10−70 nm	4:1MeOH-EtOH	8.0−10.5	13.7−18.4		152	242
nanowire[g]	w: 50−100 nm	neon	13.7	24.1	0.6	208	334
	l:3−4 μm						

[a] P_i and P_c indicate the starting and completing pressures of the phase transition, respectively. [b] Ref 24. [c] Ref 18. [d] Ref 14. [e] Ref 21. [f] Ref 16. [g] This work.

corresponding bulk material in general, as shown in Table 1. Then, the B4 and B1 phases coexisted when compressed, even to 22.4 GPa. The Rietveld analysis (Figure 3 a) indicates that at this pressure the initial B4 phase still has a significant abundance of ∼35%. Upon further compression, the wurtzite-to-rocksalt phase transition was completed at 24.1 GPa, as suggested by the disappearance of all diffraction reflections associated with the B4 phase. We note that both the onset and especially the completion pressure for the wurtzite-to-rocksalt transition are higher for ZnO nanowires in the current study than those for bulk or nanocrystal ZnO previously studied (Table 1). The ZnO nanowires were found to maintain the pure B1 phase up to 26 GPa, the highest pressure achieved in this study. The rocksalt phase was reported to persist up to 200 GPa before undergoing another phase transition.[29,30] Therefore, no further compression was carried out.

The differences in the pressure-induced phase transitions between nanostructured and bulk materials have also been observed in other materials with either enhanced or reduced transition pressures. Transition pressure enhancement has been observed in many nanomaterials, such as nanocrystal (e.g., CdSe,[31] ZnS,[32] and PbS[33]) and 1D nanomaterials (e.g., GaN nanowire,[10] SnO_2 nanowire and nanobelt,[11] ZnO nanotube,[16] and BN nanotube[12]). However, some oxide nanocrystals, such as CeO_2[34] and γ-Fe_2O_3,[35] exhibited reduced transition pressures. According to Jiang et al.,[21] such variations of transition pressure can be generally understood by examining the contributing thermodynamic functions. The driving force of the structural transformation characterized by the change in Gibbs free energy, ΔG, between the involved phases, can be interpreted as the change of three components: the ratio of volume collapse ($P\Delta V$), the surface energy difference ($A\Delta\gamma$), and the internal energy difference (ΔU).[11] In most cases mentioned above, the internal energy difference can be negligible for transitions involving solid phases. A larger ratio of volume collapse is typically associated with the reduction in the transition pressure,[35] whereas increasing surface energy can contribute to the enhancement of transition pressure.[21] As a result, the directions in which the transition pressures shift would be mainly determined by the competition between the volume collapse and surface energy difference. In all high-pressure studies of ZnO, a volume collapse was estimated to be around 16.5% at the transition pressure regardless of the morphologies.[21] Thus, the component of the ratio of volume collapse can be considered to contribute to the overall ΔG negligibly. Therefore, it can be inferred that the surface energy difference would be the dominant factor leading to variations in the transition pressures of ZnO in different forms. From Table 1, the enhanced transition pressures were observed for both nanocrystals and nanowires, and the values varied with the morphology and grain size among these nanomaterials. The above analysis suggests that the surface energy increase in nanocrystals and nanowires is associated with both the grain size and nanomorphologies. After all, it can be inferred from the relative transition pressures that the surface energy increases from nanocrystals of a large size (e.g., 50 nm) to nanowires (<100 nm) and then to nanocrystals with a small size (e.g., 12 nm).

In addition, the much higher completion pressure P_c for B4-to-B1 phase transition (i.e., 24.1 GPa) can be attributed to the pressure-induced morphology tuning effect.[10] Even with a pressure-transmitting medium (i.e., the neon), the morphology of the nanomaterial can be modified by the pressure, resulting in a broader distribution in morphology and dimensions than the starting nanomaterials upon compression. The SEM images taken before and after the compression (Figure 1a,b) revealed that some ZnO nanowires were converted to smaller nanoparticles under the compression. The modification of the morphology with a broadened size (and thus surface energy) distribution in ZnO nanowires could contribute to the extended phase stability region for the B4 phase and thus the B4−B1 coexistence region. Remarkably, it is noticed that a large number of the recovered nanowires still preserve the wire shape (Figure 1 b), in strong contrast to many other metal oxide or nitride nanowires whose morphologies were subject to substantial pressure modifications.[10,11] Such preserved wire morphology together with the larger bulk modulus (discussed later) implies the extreme toughness of the ZnO nanowires.

The backward phase transformation was also investigated. Upon decompression, the B1 phase was found to persist to 0.6 GPa characterized by the reflections exclusively associated with this phase (Figure 2). Then, the recovery of the B4 phase was only observed below 0.6 GPa or at near ambient pressure, as shown by some reflections associated with the B4 phase in the diffraction pattern of the recovered material (Figure 2). Compared with the forward transition pressure of 14.7 GPa, the much lower back transformation pressure indicates a large hysteresis for the pressure-induced transformations of ZnO nanowires. Such large hysteresis suggests that the high-pressure B1 phase is a metastable phase because prominent hysteresis was typically

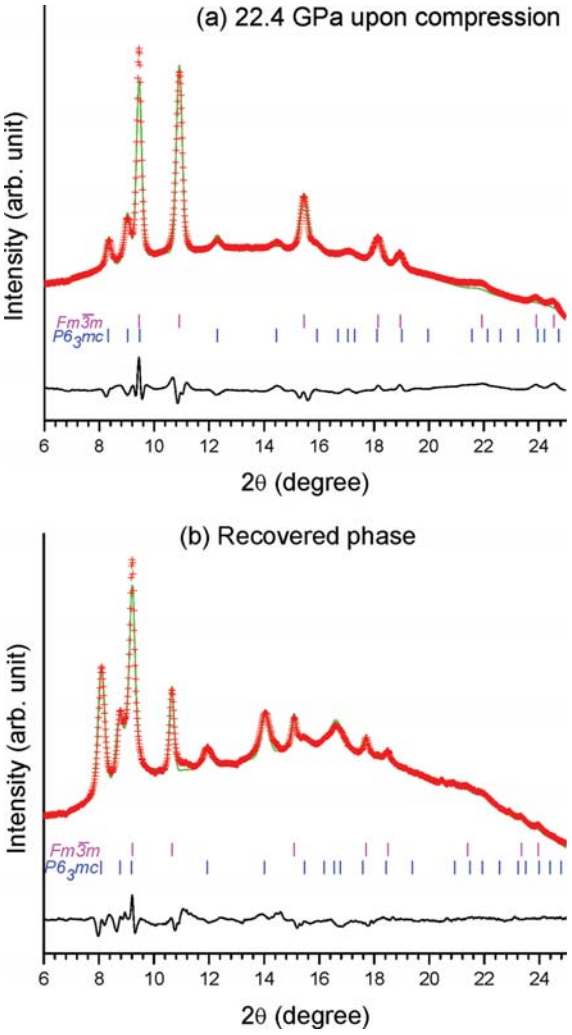

Figure 3. Rietveld refinement of XRD patterns at 22.4 GPa upon compression (a) and the recovered phase (b). The red cross is experimental X-ray intensity, whereas the green solid line is the calculated diffraction pattern based on refinement with the black curve at the bottom showing the difference between the calculated and observed intensities. The vertical bars with different colors indicate the characteristic reflections of different phases labeled in the front.

associated with different kinetic barriers that impede the sharp transition often involving a metastable phase.[10,11] Moreover, as indicated in Table 1, the backward transition pressure of 0.6 GPa was significantly lower than that observed in bulk materials and nanocrystals (i.e., 2.0[23,36] and 1.7 GPa,[21] respectively). In addition, the B4-to-B1 phase transition is completely reversible for bulk ZnO.[23,36] However, in both nanocrystals[21] and nanowires, the metastable B1 phase can still be detected in the recovered sample as a mixture with the B4 phase. Especially for the ZnO nanowire, the Rietveld refinement (Figure 3b) shows that the B1 phase still has an abundance of ~10%. All of these observations strongly demonstrate the possibility of producing specific structures or phases by combined pressure−morphology tuning.

The compression curves of the ZnO nanowire for the B4 and B1 phases were plotted in Figure 4 in comparison with those for the ZnO nanocrystals and their bulk counterparts previously studied.[14,16,18,24] By fitting the third-order Birch−Murnaghan equation of state, the bulk moduli (B_0) of the B4 and B1 phases

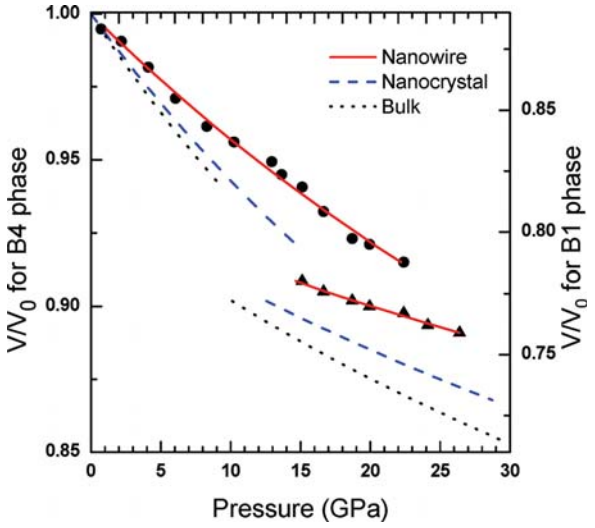

Figure 4. Pressure dependence of the unit cell volume for ZnO nanowire at room temperature in comparison with those for bulk and nanocrystals. Solid circles (B4 phase) and triangles (B1 phase) are the experimental data points obtained from this work. The solid lines represent fits to the Birch−Murnaghan equation of state. Dashed lines and dotted lines are the EOS for nanocrystals and bulk materials from refs 22 and 15, respectively.

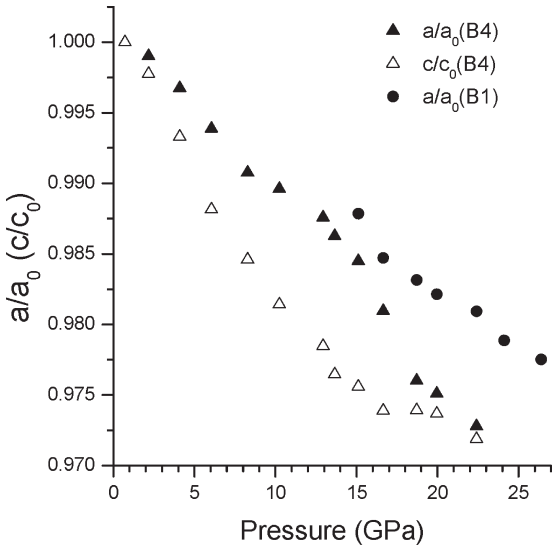

Figure 5. Cell parameter ratio as a function of pressure for ZnO nanowire. Solid and opened triangle symbols represent the a/a_0 and c/c_0 for the B4 phase, respectively. The solid circles are the a/a_0 ratio for the B1 phase.

for the ZnO nanowire were determined to be 208 and 334 GPa, respectively, with the first derivative (B_0') being fixed at 4. As can be seen, the bulk moduli of both the B4 and B1 phases are significantly larger than those for nanocrystals (i.e., 151 and 221 GPa)[14] and their bulk counterparts (i.e., 135 and 178 GPa).[18] In particular, for the high-pressure B1 phase, the ZnO nanowire exhibited a 47% enhancement in the bulk modulus compared with that for bulk ZnO. Such a size- and morphology-induced enhancement of ZnO nanowire stiffness can be understood in parallel with other nanomaterials. For example, CeO_2 and γ-Fe_2O_3 nanoparticles

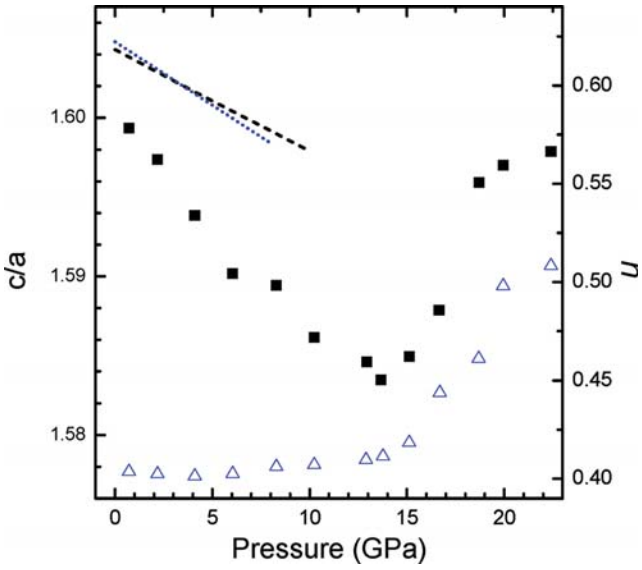

Figure 6. Pressure dependence of c/a ratio (solid squares, left vertical axis) and the internal structural parameter u of wurtzite structure ZnO (open triangles, right vertical axis) as a function of pressure obtained from Rietveld refinement. The lines show the results from refs 10 (dashed line) and 21 (dotted line), respectively.

exhibited the same enhancement of the bulk modulus compared with the bulk materials,[35,37] whereas no obvious difference in compressibility was observed for ZnS nanocrystals.[32] In contrast, the compressibility of PbS and γ-Al_2O_3 was found to increase with decreasing nanoparticle size. Furthermore, a strongly contrasting compressibility was observed for TiO_2 nanoparticles; that is, the bulk modulus of the rice-shape particles was reduced, whereas that of the rod-shaped particles was enhanced by >50% relative to that of the bulk materials.[38] Therefore, multiple factors contribute to the mechanical properties of nanomaterials. In this case, the individual ZnO nanowires can be considered to be single crystals with a strictly 1D morphology that carries very few or no defects.[28] The high crystallinity and defect-free nature of the nanowires may contribute to the enhanced mechanical properties. A similar scenario was also observed in SnO_2 nanowires.[11]

To understand the phase transition mechanism, we first plotted the a/a_0 and c/c_0 ratios for the B4 phase as a function of pressure in Figure 5, where a_0 and c_0 represent the ambient-pressure unit cell parameters. It can be seen that the c axis exhibits a higher degree of pressure dependence (0.0070 Å/GPa) than the a axis (0.0041 Å/GPa) before the onset pressure for the B4-to-B1 transition, indicating that the pressure-induced lattice deformation was more prominent along the c axis. Moreover, from the pressure dependence of the c/a axial ratio for the B4 phase depicted in Figure 6, a turning point was observed at 14 GPa, coincidental with the onset of the B4-to-B1 phase transition. Below this point, the c/a ratio follows an obvious decreasing trend and then abruptly increases with compression until the transformation is complete. In Figure 6, the internal structural parameter u obtained from the Rietveld refinements was plotted as a function of pressure. This parameter u is an atomic coordinate along the c axis for oxygen atoms residing on the Wyckoff position (1/3, 2/3, u) in space group $P6_3mc$, which defines the relative position of the two sublattices in the hexagonal wurtzite structure. Therefore, the pressure dependence of the u value could serve as the path indicator of the structural change. As indicated in Figure 6, the u value remains almost constant with a very minor decrease below 4 GPa and then increases slightly to 0.411 at 14 GPa. Thereafter, the u values increase quickly up to ~0.508 at 22 GPa, beyond which the B4 phase converts to the B1 phase completely.

These results help to evaluate the previously proposed phase transformation models. As suggested by Saitta and Decremps,[39] the B4 phase can be converted to the B1 phase via a tetragonal path via an intermediate tetragonal phase characterized with each Zn (or O) atom located at the body center of the square pyramid formed by five O (or Zn) atoms. The c/a and u remain close to that of the B4 structure first; then, the c/a ratio decreases to bring the Zn atom from the body center to the base center of the pyramid until u = 0.5, resulting in the B1 structure. However, Limpijumnong and Jungthawa[40] proposed an alternative model that the B4-to-B1 phase transition could follow a hexagonal path. In this model, the c/a ratio first decreases continuously, whereas the u increases to 0.5. Then the γ angle (60°) opens up to 90°, and the B1 phase forms eventually. In this work, the c/a ratio was observed to decrease monotonically with compression before the transition started. Although the u values exhibited no obvious increase below 4 GPa, the overall trend still demonstrated an increase in the u value with pressure, suggesting that the B4-to-B1 phase transformation in the ZnO nanowire is more likely via the hexagonal rather than the tetragonal path. This hexagonal model was also proposed for other ZnO materials, such as nanocrystals,[14] nanotubes,[16] and their corresponding bulk counterparts,[18] as indicated by either the changes of the c/a ratio or the u values. Therefore, our results indicate that the transformation path for the B4-to-B1 of ZnO is independent of the morphologies or one-dimensionality.

CONCLUSIONS

In summary, we have investigated the high-pressure structures and properties of the 1D nanostructured ZnO using synchrotron X-ray diffraction. The B4-to-B1 phase transformation was found to start at 13.7 GPa and to complete at 24.1 GPa, the highest completion pressure for the B4-to-B1 phase transformation observed in ZnO so far. Upon decompression, the pure high-pressure B1 phase was found to persist down to 0.6 GPa. Bulk moduli for the B4 and B1 phases were determined to be 208 and 334 GPa, respectively, both of which were drastically enhanced as compared with ZnO in other morphologies. Aided by the SEM images, the combined pressure-morphology effects on ZnO wires can be understood based on other nanostructured materials previously studied. Finally, the pressure dependence of both the unit cell parameter c/a ratio and the structure parameter u strongly suggests the B4-to-B1 phase transition for ZnO nanowire via the hexagonal path.

AUTHOR INFORMATION

Corresponding Author

*E-mail: yang.song@uwo.ca. Phone: (519)661-2111, ext. 86310. Fax: (519)661-3022.

ACKNOWLEDGMENT

This work was supported by a Discovery Grant, a Research Tools and Instruments Grant from the Natural Science and Engineering Research Council of Canada, a Leaders Opportunity

Fund from the Canadian Foundation for Innovation, and an Early Researcher Award from the Ontario Ministry of Research and Innovation. We acknowledge Dr. S. Sinogeikin at HPCAT and Dr. S. Tkachev at GSECARS for their technical assistance. This work was performed at HPCAT (Sector 16), Advanced Photon Source (APS), Argonne National Laboratory. HPCAT is supported by CIW, CDAC, UNLV, and LLNL through funding from DOE-NNSA, DOE-BES, and NSF. APS is supported by DOE-BES, under contract no. DE-AC02-06CH11357. S.J., S.A.M., and L.L. thank the support by US NSF (DMR-0548232, DMR-1106184, and DMR-0832760).

REFERENCES

(1) Minne, S. C.; Manalis, S. R.; Quate, C. F. *Appl. Phys. Lett.* **1995**, *67*, 3918.
(2) Gorla, C. R.; Emanetoglu, N. W.; Liang, S.; Mayo, W. E.; Lu, Y.; Wraback, M.; Shen, H. *J. Appl. Phys.* **1999**, *85*, 2595.
(3) Huang, Y. H.; Zhang, Y.; Gu, Y. S.; Bai, X. D.; Qi, J. J.; Liao, Q. L.; Liu, J. *J. Phys. Chem. C* **2007**, *111*, 9039.
(4) Huang, M. H.; Mao, S.; Feick, H.; Yan, H. Q.; Wu, Y. Y.; Kind, H.; Weber, E.; Russo, R.; Yang, P. D. *Science* **2001**, *292*, 1897.
(5) Hullavarad, S.; Hullavarad, N.; Look, D.; Claflin, B. *Nanoscale Res. Lett.* **2009**, *4*, 1421.
(6) Wang, X. D.; Song, J. H.; Liu, J.; Wang, Z. L. *Science* **2007**, *316*, 102.
(7) Cheng, H. M.; Hsu, H. C.; Tseng, Y. K.; Lin, L. J.; Hsieh, W. F. *J. Phys. Chem. B* **2005**, *109*, 8749.
(8) Lu, C. Y.; Chang, S. P.; Chang, S. J.; Hsueh, T. J.; Hsu, C. L.; Chiou, Y. Z.; Chen, C. *IEEE Sens. J.* **2009**, *9*, 485.
(9) San-Miguel, A. *Chem. Soc. Rev.* **2006**, *35*, 876.
(10) Dong, Z. H.; Song, Y. *Appl. Phys. Lett.* **2009**, *96*, 3.
(11) Dong, Z. H.; Song, Y. *Chem. Phys. Lett.* **2009**, *480*, 90.
(12) Dong, Z. H.; Song, Y. *J. Phys. Chem. C* **2010**, *114*, 1782.
(13) Shchennikov, V. V.; Ovsyannikov, S. V. *High Pressure Res.* **2009**, *29*, 514.
(14) Kumar, R. S.; Cornelius, A. L.; Nicol, M. F. *Curr. Appl. Phys.* **2007**, *7*, 135.
(15) Decremps, F.; Datchi, F.; Saitta, A. M.; Itie, J. P.; Polian, A.; Baudelet, F.; Pascarelli, S. *High Pressure Res.* **2002**, *22*, 365.
(16) Hou, D. B.; Ma, Y. Z.; Gao, C. X.; Chaudhuri, J.; Lee, R. G.; Yang, H. B. *J. Appl. Phys.* **2009**, *105*, 4.
(17) Jiang, J. Z. *J. Mater. Sci.* **2004**, *39*, 5103.
(18) Liu, H. Z.; Ding, Y.; Somayazulu, M.; Qian, J.; Shu, J.; Hausermann, D.; Mao, H. K. *Phys. Rev. B* **2005**, *71*, 4.
(19) Bates, C. H.; Roy, R.; White, W. B. *Science* **1962**, *137*, 993.
(20) Zhuravlev, K. K.; Oo, W. M. H.; McCluskey, M. D.; Huso, J.; Morrison, J. L.; Bergman, L. *J. Appl. Phys.* **2009**, *106*, 4.
(21) Jiang, J. Z.; Olsen, J. S.; Gerward, L.; Frost, D.; Rubie, D.; Peyronneau, J. *Europhys. Lett.* **2000**, *50*, 48.
(22) Wu, Z. Y.; Bao, Z. X.; Zou, X. P.; Tang, D. S.; Liu, C. X.; Dai, J. H.; Xie, S. S.; Li, Q. S.; Shen, Z. X.; Zou, B. S. *Mater. Sci. Technol.* **2003**, *19*, 981.
(23) Desgreniers, S. *Phys. Rev. B* **1998**, *58*, 14102.
(24) Karzel, H.; Potzel, W.; Kofferlein, M.; Schiessl, W.; Steiner, M.; Hiller, U.; Kalvius, G. M.; Mitchell, D. W.; Das, T. P.; Blaha, P.; Schwarz, K.; Pasternak, M. P. *Phys. Rev. B* **1996**, *53*, 11425.
(25) Recio, J. M.; Blanco, M. A.; Luana, V.; Pandey, R.; Gerward, L.; Olsen, J. S. *Phys. Rev. B* **1998**, *58*, 8949.
(26) Yan, X. Q.; Gu, Y. S.; Zhang, X. M.; Huang, Y. H.; Qi, J. J.; Zhang, Y.; Fujita, T.; Chen, M. W. *J. Phys. Chem. C* **2009**, *113*, 1164.
(27) Jin, S.; Bierman, M. J.; Morin, S. A. *J. Phys. Chem. Lett.* **2010**, *1*, 1472.
(28) Morin, S. A.; Bierman, M. J.; Tong, J.; Jin, S. *Science* **2010**, *328*, 476.
(29) Maouche, D.; Saoud, F. S.; Louail, L. *Mater. Chem. Phys.* **2007**, *106*, 11.
(30) Liu, H. Z.; Tse, J. S.; Mao, H. K. *J. Appl. Phys.* **2006**, *100*, 5.
(31) Tolbert, S. H.; Alivisatos, A. P. *Science* **1994**, *265*, 373.
(32) Jiang, J. Z.; Gerward, L.; Frost, D.; Secco, R.; Peyronneau, J.; Olsen, J. S. *J. Appl. Phys.* **1999**, *86*, 6608.
(33) Jiang, J. Z.; Gerward, L.; Secco, R.; Frost, D.; Olsen, J. S.; Truckenbrodt, J. *J. Appl. Phys.* **2000**, *87*, 2658.
(34) Rekhi, S.; Saxena, S. K.; Lazor, P. *J. Appl. Phys.* **2001**, *89*, 2968.
(35) Jiang, J. Z.; Olsen, J. S.; Gerward, L.; Morup, S. *Europhys. Lett.* **1998**, *44*, 620.
(36) Decremps, F.; Datchi, F.; Saitta, A. M.; Polian, A.; Pascarelli, S.; Di Cicco, A.; Itie, J. P.; Baudelet, F. *Phys. Rev. B* **2003**, *68*, 10.
(37) Wang, Z. W.; Zhao, Y. S.; Schiferl, D.; Zha, C. S.; Downs, R. T. *Appl. Phys. Lett.* **2004**, *85*, 124.
(38) Park, S. W.; Jang, J. T.; Cheon, J.; Lee, H. H.; Lee, D. R.; Lee, Y. *J. Phys. Chem. C* **2008**, *112*, 9627.
(39) Saitta, A. M.; Decremps, F. *Phys. Rev. B* **2004**, *70*, 035214.
(40) Limpijumnong, S.; Jungthawan, S. *Phys. Rev. B* **2004**, *70*, 054104.